High-Level, First-Principles, Full-Dimensional Quantum Calculation of the Ro-vibrational Spectrum of the Simplest Criegee Intermediate (CH_2OO)

Jun Li,[†] Stuart Carter,[‡] Joel M. Bowman,[‡] Richard Dawes,[§] Daiqian Xie,[∥] and Hua Guo*,[†]

[†]Department of Chemistry and Chemical Biology, University of New Mexico, Albuquerque, New Mexico 87131, United States
[‡]Department of Chemistry, Emory University, Atlanta, Georgia 30322, United States
[§]Department of Chemistry, Missouri University of Science and Technology, Rolla, Missouri 65409, United States
[∥]Institute of Theoretical and Computational Chemistry, Key Laboratory of Mesoscopic Chemistry, School of Chemistry and Chemical Engineering, Nanjing University, Nanjing, 210093, China

ABSTRACT: The ro-vibrational spectrum of the simplest Criegee intermediate (CH_2OO) has been determined quantum mechanically based on nine-dimensional potential energy and dipole surfaces for its ground electronic state. The potential energy surface is fitted to more than 50 000 high-level ab initio points with a root-mean-square error of 25 cm^{-1}, using a recently proposed permutation invariant polynomial neural network method. The calculated rotational constants, vibrational frequencies, and spectral intensities of CH_2OO are in excellent agreement with experiment. The potential energy surface provides a valuable platform for studying highly excited vibrational and unimolecular reaction dynamics of this important molecule.
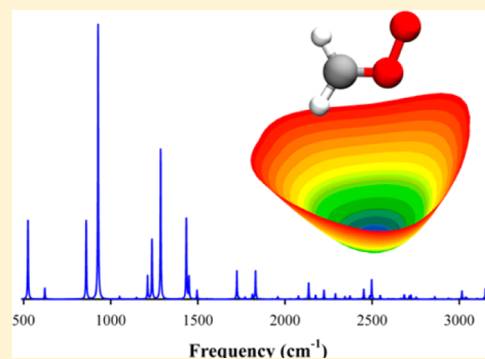
SECTION: Environmental and Atmospheric Chemistry, Aerosol Processes, Geochemistry, and Astrochemistry

Ozonolysis,[1] namely, the reactions of ozone with alkenes from either natural or man-made sources including combustion, is an important atmospheric process, leading to free radicals such as OH. The mechanism of ozonolysis is believed to start with an exothermic 1,3-cycloaddition of O_3 to the C=C double bond, leading to a primary ozonide (POZ). Predicted by Criegee in 1949, the dissociation of POZ produces an important intermediate, namely R_1R_2COO with R_1,R_2=H/ alkyl bonded directly to C.[2] Despite their importance, it is only recently that the Criegee intermediates have started to be directly detected and investigated in the gas phase,[3,4] thanks to an efficient scheme to generate such metastable species.[5] Due to the exothermic nature of the reaction, the Criegee intermediates are often produced with large amounts of internal energy and are thus highly reactive with short lifetimes. It is now established that they are involved in several important atmospheric reactions with unexpectedly rapid rates,[5-9] but can be removed via photodissociation near 340 nm, leading to O(^{1}D) and aldehydes/ketones.[10-14] As a result, they are now considered as major initiators of oxidation reactions in the atmosphere, in addition to the hydroxyl radical, particularly in winter when the photoproduction of OH is inefficient.[1,3]

To elucidate the chemical and photochemical reactions involving the Criegee intermediates, it is imperative to understand their structures as well as the vibrational and unimolecular reaction dynamics in their ground electronic states. Indeed, the simplest Criegee intermediate (CH_2OO or

formaldehyde oxide) has been argued to exist in either a biradical[15] or zwitterionic form,[16,17] which have different structural and reaction characteristics. So far, the structure of CH_2OO has been determined experimentally using microwave spectroscopy,[18-20] and its vibrational spectrum has been recorded with infrared (IR) spectroscopy.[21] Theoretical models are essential in assigning the spectroscopic features in these experiments.

The recent flurry of spectroscopic measurements has posed a challenge to theory to better understand the structure and dynamics of this important molecule. Although some ab initio calculations of CH_2OO have been reported and vibrational frequencies computed,[16,19,21-24] there has been no global potential energy surface (PES) that will allow a thorough understanding of not only its highly excited vibrational states, but also isomerization and decomposition dynamics. The only theoretical study of such unimolecular processes was done using a direct-dynamics method.[25] In this Letter, we report the first nine-dimensional PES for CH_2OO based on ~50 000 high-level ab initio points. These points were fit with the recently proposed permutation invariant polynomial neural network (PIP-NN) method,[26,27] with a root-mean square error (RMSE) of only 3.1 meV (25 cm^{-1}). Anharmonic vibrational energy

Figure 1. Correlation diagram for CH₂OO. All energies are in kcal/mol and with ZPE corrections. The values for CH₂OO, TS1, and dioxirane are calculated at the level of CCSD(T)-F12a/AVTZ; the dissociation energies for products (might with barriers) $CH_2 + O_2$ and $H_2CO + O$ are from ref 16; the energies of the methylenebis(oxy) and TS2 were obtained at the level of CASSCF(14,12)/VDZ.[22] The further isomerization of methylenebis(oxy) to the global minimum (ca. −120 kcal/mol) formic acid HCOOH is not shown. The geometry of CH₂OO (lengths in angstroms and angles in degrees) is given in the inset and the numbers from top are for the fitted PES, CCSD(T)-F12a/AVTZ, CCSD(T)-F12/AV5Z,[18] CCSD(T)/aug-cc-pCV5Z with ΔT and ΔQ corrections,[19] and the empirical ("semi-experimental") equilibrium structures.[19]

Table 1. Comparison of the Fundamental Vibrational Frequencies (cm⁻¹) of CH₂OO

mode	sym.	description	expt.[a]	this work[b]			NEVPT2[c]		CAS HO[d]	CCSD(T) HO[e]	CCSD(T) HO[f]
				VCI-5	PES (HO)	ab initio (HO)	HO	AHO			
ν_1	A′	C−H antisym. str.	-	3151	3300	3302	3370	3149	3215	3290	3302
ν_2	A′	C−H sym. str.	-	3013	3137	3141	3197	3030	3065	3137	3140
ν_3	A′	CH₂ scissor	1435	1434	1488	1490	1500	1458	1465	1483	1489
ν_4	A′	CO str./CH₂ scissor	1286	1285	1321	1317	1338	1302	1269	1306	1316
ν_5	A′	CH₂ rock	1241	1212	1241	1240	1235	1220	1233	1231	1239
ν_6	A′	OO str.	908	927	949	951	916	892	849	935	945
ν_7	A′	COO deform	-	526	536	536	536	530	537	529	532
ν_8	A″	CH₂ wag	848	859	872	878	856	853	793	862	876
ν_9	A″	CH₂ twist	-	622	642	639	620	606	618	632	651

[a]Experimental frequencies.[21] [b]This work: VCI with up to 5-mode excitations; PES (HO) and ab initio (HO) for harmonic frequencies on the fitted PES and calculated at the CCSD(T)-F12a/AVTZ level. [c]NEVPT2/AVDZ: HO for harmonic frequencies; AHO for anharmonic frequencies.[21] [d]Harmonic frequencies at CAS(14,12)/VDZ.[22] [e]Harmonic frequencies at CCSD(T)/AVTZ.[23] [f]Harmonic frequencies at CCSD(T)/A′VQZ.[24]

levels and wave functions were obtained on this new PES using the MULTIMODE approach.[28] In addition, the IR spectrum has been generated using a new fitted dipole surface with all nine coordinates.

The PES of the CH₂O₂ system is quite complicated, including isomers such as formaldehyde oxide (namely CH₂OO), dioxirane, dihydroxycarbene, formic acid, and various products such as HCO, OH, CO₂, H₂, CO, H₂O, O, H₂CO, etc. We focus here on the region near the CH₂OO(X^1A') local minimum (see Figure 1). To this end, we have used an explicitly correlated (F12) coupled cluster method with singles, doubles, and perturbative triples with the augmented correlation-consistent polarized valence triple-ζ basis set (CCSD(T)-F12a/AVTZ),[29,30] which has been shown to produce results close to the conventional CCSD(T) complete basis set (CBS) limit. The optimized geometry of CH₂OO and harmonic frequencies at the CCSD(T)-F12a/AVTZ level are

very close to available theoretical and experimental results (*vide infra*). These calculations were performed with MOLPRO.[31] We note in passing that there are a small number of points with large T_1 diagnostic values at high energies, and they have been excluded from our data set for fitting the PES.

As shown in Figure 1, a barrier (TS1, imaginary frequency 755.49 cm⁻¹) divides CH₂OO and dioxirane. At the CCSD(T)-F12a/AVTZ level, the barrier is 19.98 kcal/mol, or 18.98 kcal/mol with zero point energy (ZPE) corrections. These values are very close to the latest theoretical results.[25] In Figure 1, the calculated geometry of the CH₂OO molecule is compared with both experiment and previous theoretical results and the agreement is excellent. Noting the significantly shorter C−O bond than the O−O bond, our results concur with the recent consensus[19,21] that this molecule is closer to the zwitterionic, rather than biradical, form. The calculated harmonic vibrational

Figure 2. (a) Contour plots along the bond lengths O−O (*x*-axis) and C−O (*y*-axis), other coordinates optimized within a plane. (b) Contour plots along the COO bond angle (*x*-axis) and the HCOO dihedral angle (*y*-axis) with other coordinates optimized. (c) Fitting errors ($E_{fit} − E_{ab}$, in eV) as a function of the ab initio energies (in eV). Energies in (a) and (b) are in kcal/mol. A and C denote the potential minima for CH_2OO and its cyclic isomer dioxirane, with B as the transition state (TS1).

frequencies are listed in Table 1 with previous experimental and theoretical data.

In order to provide an accurate PES with reasonable computational costs, it is vital to choose the distribution of the ab initio points prudently. Following our earlier

strategies,[32−34] we first determined a set of geometries near the CH_2OO equilibrium by running direct-dynamics trajectories (in particular, the Atomic Centered Density Matrix Propagation molecular dynamics model implemented in Gaussian 09[35] was employed) at the B3LYP/6-31+G(d, p) level. These geometries were screened to remove points that are too close to each other, using the Euclidean criteria $\chi = (\sum_i^{10} (r_i - r_i^{new})^2)^{1/2} < 0.1$ Å where r_i is the internuclear distance. Although CH_2OO has several decomposition and isomerization channels, configurations far from its equilibrium geometry are excluded in this work. Note that due to the permutation symmetry, each configuration actually corresponds to four sets of internuclear distances, and all are considered in the screening. The CCSD(T)-F12a/AVTZ calculations were then carried out and the results were fit to a primitive PES. To further explore the topography of the PES, batches of classical trajectories with different energies were run, and additional geometries were chosen using the same protocol described above. This procedure was iterated multiple times until the results were converged.

In total, 50 459 points were calculated. The PES was constructed with the PIP-NN method,[26,27] which has shown excellent performance in fitting PESs for several 4- and 5-atom systems.[27,36−38] Briefly, the input layer of the NN consists of low-order PIPs, which are symmetrized monomials,[39]

$$\mathbf{G} = \hat{\mathbf{S}} \prod_{i<j}^{N} p_{ij}^{l_{ij}} \tag{1}$$

where $p_{ij} = \exp(−ar_{ij})$ are the Morse-like variables with a as an adjustable constant and r_{ij} the $N(N − 1)/2$ (here $N = 5$) internuclear distances.[32] l_{ij} is the degree of p_{ij} and $M = \sum_{i<j}^{N} l_{ij}$ is the total degree in each monomial. $\hat{\mathbf{S}}$ is the symmetrization operator, which consists of all possible nuclear permutation operations in the system. This direct symmetrization has been developed previously, without NN fitting, by Bowman and co-workers.[32] It is worth noting that the number of PIPs in the input layer should be sufficiently large to ensure the permutation symmetry of the system.[27] For this system, we have included all 101 PIPs up to third order.

The explicit form of the basis functions in the neurons can be found in refs 26−27 and thus are not repeated here. Several different NN structures with one or two hidden layers were tested. We settled on two hidden layers with N_1 and N_2 neurons, respectively. In each NN fitting, the data were divided randomly into three sets, namely the training (90% of the data points), validation (5%), and test (5%) sets. All NN fittings were performed using the Levenberg−Marquardt algorithm with the following root-mean-square error (RMSE):

$$\text{RMSE} = \sqrt{\sum_{i=1}^{N_{data}} w(E_i^{output} − E_i^{target})^2 / N_{data}} \tag{2}$$

where w is the weighting function that assigns a factor of 5 for energy points below 0.8 eV while unity for others, and E_i^{target} and E_i^{output} are the input and fitted energies, respectively. To avoid false extrapolation due to edge points in the randomly selected validation and test sets, only fits with similar RMSEs for all three sets were accepted. In addition, the maximum deviation is also used in selecting the final PIP-NN fits. For each architecture, 50 different training calculations were performed, and the "early stopping" method[40] was used to avoid over fitting. The training method converges quickly for all

Table 2. Pure Rotational Transition Frequencies between Different $J_{K_aK_c}$ States (in cm^{-1}) of CH$_2$OO

$1_{01}-0_{00}$		$2_{02}-1_{01}$		$1_{10}-1_{01}$		$1_{11}-2_{02}$	
expt.[a]	theo.[b]	expt.[a]	theo.[b]	expt.[a]	theo.[b]	expt.[a]	theo.[b]
0.7734	0.7721	1.5457	1.5432	2.2357	2.2291	0.6319	0.6127

[a]Experiment.[18] [b]This work, theoretical calculations.

Table 3. Rotational Constants for Several Isotopomers of CH$_2$OO

	A_0		B_0		C_0	
	expt.[a]	theo.[b]	expt.[a]	theo.[b]	expt.[a]	theo.[b]
H$_2$COO	2.5934	2.6005	0.4158	0.4182	0.3576	0.3603
H$_2$^{13}COO	2.5709	2.5777	0.4033	0.4056	0.3479	0.3505
H$_2$C^{18}OO	2.4482	2.4537	0.4158	0.4181	0.3547	0.3573
H$_2$CO^{18}O	2.5646	2.5715	0.3928	0.3951	0.3400	0.3425
D$_2$COO	2.0191	2.0257	0.3693	0.3712	0.3116	0.3137
d$_1$,trans-HDCOO	2.5563	2.5639	0.3773	0.3794	0.3282	0.3305
d$_1$,cis-HDCOO	2.0604	2.0672	0.4048	0.4069	0.3376	0.3400
D$_2$C^{18}O^{18}O	1.9026	1.9081	0.3491	0.3508	0.2944	0.2963
H$_2$C^{18}O^{18}O	2.4180	2.4234	0.3926	0.3948	0.3371	0.3395

[a]Reference 19, while other experimental numbers[18,20] are very close. [b]This work, theoretical calculations, computed from the same minimum structure.
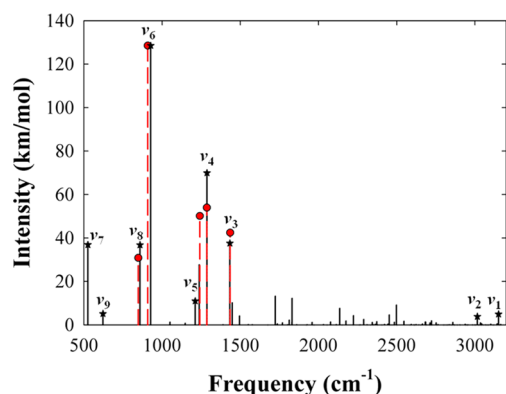
Figure 3. Comparison of the IR spectrum of CH$_2$OO obtained from experiment[21] (in dashed red) and theory (in solid black), in which the experimental values are normalized with the intensity of the ν_6 line. The fundamentals are all indicated by additional symbols (circles or stars for experiment or theory).

the fitting reported here, typically finishing within a few hundred steps. The final PIP-NN PES was chosen as the average of three best fits.

The final fits have a NN structure of 10 and 40 interconnected neurons in the two hidden layers with 1501 parameters and the three best PIP-NN fits have RMSEs for train/valid/test sets and the maximum deviation of 3.8/4.4/6.0/197.8, 4.0/4.5/5.2/111.3, and 3.2/4.6/5.5/188.8 meV, respectively. The RMSE of the averaged PIP-NN PES is 3.1 meV, and the maximum deviation is 87.6 meV. The ab initio equilibrium geometry and harmonic frequencies are well reproduced by the PES, as shown in Figure 1 and Table 1. In Figure 2, contour plots are displayed in two pairs of coordinates. In panel a, the potential minimum is clearly seen, and the elongation of the O−O or C−O bonds eventually leads the O + CH$_2$O or CH$_2$ + O$_2$ dissociation limit. In panel b, the potential rises steeply along the dihedral angle (ϕ), consistent with a C=O double bond. In addition, the transition state (TS1) between formaldehyde oxide (CH$_2$OO) and the cyclic

dioxirane (CH$_2$O$_2$) is clearly seen. Finally, the fitting errors of all the data points are shown in panel c of the same figure.

The permanent dipole of CH$_2$OO was computed to be 4.11 D at the CCSD(T)-F12a/AVDZ level, comparable to 3.97 D calculated at a similar level by Cremer et al.[16] A total of 45743 points in the CH$_2$OO well were computed and fit to a point-charge expression using the PIP method.[41] 1122 parameters were used for each component of the dipole moment, and the RMSEs of the fits are 0.027, 0.007, and 0.003 D for the x, y, z components, respectively. Note that the dipole moment is related to the coordinate origin, and all the sampled points were in the principal axis frame.

The ro-vibrational energy levels of CH$_2$OO on this new PES were determined using the MULTIMODE approach[28] based on the Watson Hamiltonian.[42] Since it has been discussed extensively in the literature, few details are given here. It suffices to say that mass-scaled normal mode coordinates are used in the Hamiltonian. The vibrational wave function is written as an expansion of direct-product basis functions, while the potential is expanded with a hierarchical n-mode representation. The calculations were done with a truncated potential with up to 6-mode terms. The $J = 0$ vibrational problem was first solved using the vibrational self-consistent field (VSCF) approach.[43,44] To account for coupling among the nine vibrational modes, we go beyond the VSCF approximation by expanding the vibrational wave function in terms of the eigenfunctions of the VSCF Hamiltonian. This virtual configuration interaction (VCI) method[45,46] typically improves the results, and is used here with up to 5-mode excitations. Convergence tests suggest that the vibrational frequencies are converged to ~2 cm^{-1}. For $J > 0$, the basis for the VCI calculations is a direct product of the VSCF basis and symmetric top wave functions $|JK0\rangle$, and the ro-vibrational levels are obtained by diagonalization of the corresponding Hamiltonian matrix.[46] The intensities were computed using the method described in ref 47.

In Table 1, the $J = 0$ calculated VCI anharmonic vibrational frequencies on the PES are compared with both experimental and previous theoretical values. The agreement with the experimental data of Su et al.[21] is quite satisfactory. We note

that the experimental value for the ν_5 (CH_2 rock) mode (1241 cm^{-1}) is possibly misassigned, and a new value is expected to be smaller (Y.-P. Lee, private communication), and thus closer to our prediction. The only large error is found for the O−O stretching frequency, which corresponds to the asymmetric stretching mode of the isoelectronic O_3. The asymmetric stretching frequency in ozone is challenging to calculate accurately and is sensitive to higher-order electron correlation. MRCI(Q)/CBS overshoots ν_3 by roughly 30 cm^{-1} while still underestimating D_e. Higher-order correlation is needed to soften the well, yet increase D_e.[48−50] Watts and Bartlett found that for single reference coupled cluster methods the effect of adding triple excitations contributed changes in the harmonic stretching frequency ω_3 (ozone) of more than 100 cm^{-1}, a dramatic effect of high-order correlation.[51] Given the similarities to the complicated electronic structure of ozone, we consider the performance of the CCSD(T)-F12a/AVTZ method to be remarkably good for CH_2OO.

Calculated pure rotational excitation frequencies for the ground vibrational state of CH_2OO are compared in Table 2 with available experimental data.[18] The agreement is quite satisfactory. In Table 3, the calculated rotational constants for several isotopomers of CH_2OO are listed along with the values derived from measurements.[18−20] Again, the agreement is excellent.

In Figure 3, the calculated IR spectrum for CH_2OO is displayed, with comparison with the experimental spectral positions and relative intensities. The latter was normalized with the ν_6 feature. It is clear that the agreement is quite satisfactory. It should be noted that the experimental spectrum is restricted to a region between 800 and 1500 cm^{-1}. As a result, some strong features predicted by our calculations have not been observed, thus serving as predictions. In addition, the calculated ν_5 feature has a much smaller intensity than reported by the experiment, which supports the notion that this line might have been misassigned. As shown in the figure, the experimental frequency (1241 cm^{-1}) is very close to a relatively strong feature in the calculated spectrum, which was assigned to be $2\nu_9$ (1237 cm^{-1}), which borrows some intensity from ν_4 through mode mixing.

To summarize, we have constructed a full nine-dimensional highly accurate semiglobal PES for the simplest Criegee intermediate (CH_2OO) and the dipole surface. They allowed us to determine the vibrational spectrum and rotational constants. Agreement with the available experimental data is generally excellent, and the theoretical predictions are expected to help sort out the assignment of the experimental spectral features. This PES will also provide a solid foundation for further studies of the highly excited vibrational spectrum as well as unimolecular and photochemical reactions in this important system.

■ AUTHOR INFORMATION

Corresponding Author
*E-mail: hguo@unm.edu.

Notes
The authors declare no competing financial interest.

■ ACKNOWLEDGMENTS

■ REFERENCES

(1) Johnson, D.; Marston, G. The Gas-Phase Ozonolysis of Unsaturated Volatile Organic Compounds in the Troposphere. *Chem. Soc. Rev.* **2008**, *37*, 699−716.

(2) Criegee, R. Mechanism of Ozonolysis. *Angew. Chem., Int. Ed.* **1975**, *14*, 745−752.

(3) Taatjes, C. A.; Shallcross, D. E.; Percival, C. J. Research Frontiers in the Chemistry of Criegee Intermediates and Tropospheric Ozonolysis. *Phys. Chem. Chem. Phys.* **2014**, *16*, 1704−1718.

(4) Vereecken, L.; Francisco, J. S. Theoretical Studies of Atmospheric Reaction Mechanisms in the Troposphere. *Chem. Soc. Rev.* **2012**, *41*, 6259−6293.

(5) Welz, O.; Savee, J. D.; Osborn, D. L.; Vasu, S. S.; Percival, C. J.; Shallcross, D. E.; Taatjes, C. A. Direct Kinetic Measurements of Criegee Intermediate (CH_2OO) Formed by Reaction of CH_2I with O_2. *Science* **2012**, *335*, 204−207.

(6) Taatjes, C. A.; Welz, O.; Eskola, A. J.; Savee, J. D.; Scheer, A. M.; Shallcross, D. E.; Rotavera, B.; Lee, E. P. F.; Dyke, J. M.; Mok, D. K. W.; Osborn, D. L.; Percival, C. J. Direct Measurements of Conformer-Dependent Reactivity of the Criegee Intermediate CH_3CHOO. *Science* **2013**, *340*, 177−180.

(7) Kjaergaard, H. G.; Kurten, T.; Nielsen, L. B.; Jorgensen, S.; Wennberg, P. O. Criegee Intermediates React with Ozone. *J. Phys. Chem. Lett.* **2013**, *4*, 2525−2529.

(8) Taatjes, C. A.; Welz, O.; Eskola, A. J.; Savee, J. D.; Osborn, D. L.; Lee, E. P. F.; Dyke, J. M.; Mok, D. W. K.; Shallcross, D. E.; Percival, C. J. Direct Measurement of Criegee Intermediate (CH_2OO) Reactions with Acetone, Acetaldehyde, and Hexafluoroacetone. *Phys. Chem. Chem. Phys.* **2012**, *14*, 10391−10400.

(9) Su, Y. T.; Lin, H.-Y.; Putikam, R.; Matsui, H.; Lin, M. C.; Lee, Y. P. Extremely Rapid Self-Reaction of the Simplest Criegee Intermediate CH_2OO and Its Implications in Atmospheric Chemistry. *Nat. Chem.* **2014**, *6*, 477−483.

(10) Beames, J. M.; Liu, F.; Lu, L.; Lester, M. I. Ultraviolet Spectrum and Photochemistry of the Simplest Criegee Intermediate CH_2OO. *J. Am. Chem. Soc.* **2012**, *134*, 20045−20048.

(11) Lehman, J. H.; Li, H.; Beames, J. M.; Lester, M. I. Communication: Ultraviolet Photodissociation Dynamics of the Simplest Criegee Intermediate CH_2OO. *J. Chem. Phys.* **2013**, *139*, 141103.

(12) Beames, J. M.; Liu, F.; Lu, L.; Lester, M. I. UV Spectroscopic Characterization of an Alkyl Substituted Criegee Intermediate CH_3CHOO. *J. Chem. Phys.* **2013**, *138*, 244307.

(13) Sheps, L. Absolute Ultraviolet Absorption Spectrum of a Criegee Intermediate CH_2OO. *J. Phys. Chem. Lett.* **2013**, *4*, 4201−4205.

(14) Ting, W.-L.; Chen, Y.-H.; Chao, W.; Smith, M. C.; Lin, J. J. The UV Absorption Spectrum of the Simplete Criegee Intermediate CH_2OO. *Phys. Chem. Chem. Phys.* **2014**, *16*, 10438−10443.

(15) Wadt, W. R.; Goddard, W. A. The Electronic Structure of the Criegee Intermediate. Ramifications for Mechanism of Ozonolysis. *J. Am. Chem. Soc.* **1975**, *97*, 3004−3021.

(16) Cremer, D.; Gauss, J.; Kraka, E.; Stanton, J. F.; Bartlett, R. J. A CCSD(T) Investigation of Carbonyl Oxide and Dioxirane - Equilibrium Geometries, Dipole Moments, Infrared Spectra, Heats of Formation and Isomerization Energies. *Chem. Phys. Lett.* **1993**, *209*, 547−556.

(17) Anglada, J. M.; Bofill, J. M.; Olivella, S.; Sole, A. Unimolecular Isomerizations and Oxygen Atom Loss in Formaldehyde and Acetaldehyde Carbonyl Oxides. A Theoretical Investigation. *J. Am. Chem. Soc.* **1996**, *118*, 4636−4647.

(18) Nakajima, M.; Endo, Y. Communication: Determination of the Molecular Structure of the Simplest Criegee Intermediate CH₂OO. *J. Chem. Phys.* 2013, *139*, 101103.

(19) McCarthy, M. C.; Cheng, L.; Crabtree, K. N.; Martinez, O.; Nguyen, T. L.; Womack, C. C.; Stanton, J. F. The Simplest Criegee Intermediate (H₂C=O−O): Isotopic Spectroscopy, Equilibrium Structure, and Possible Formation from Atmospheric Lightning. *J. Phys. Chem. Lett.* 2013, *4*, 4133−4139.

(20) Daly, A. M.; Drouin, B. J.; Yu, S. Submillimeter Measurements of the Criegee Intermediate CH₂OO in the Gas Phase. *J. Mol. Spectrosc.* 2014, *297*, 16−20.

(21) Su, Y. T.; Huang, Y. H.; Witek, H. A.; Lee, Y. P. Infrared Absorption Spectrum of the Simplest Criegee Intermediate CH₂OO. *Science* 2013, *340*, 174−176.

(22) Fang, D. C.; Fu, X. Y. CASSCF and CAS+1+2 Studies on the Potential Energy Surface and the Rate Constants for the Reactions between CH₂ and O₂. *J. Phys. Chem. A* 2002, *106*, 2988−2993.

(23) Nguyen, M. T.; Nguyen, T. L.; Ngan, V. T.; Nguyen, H. M. T. Heats of Formation of the Criegee Formaldehyde Oxide and Dioxirane. *Chem. Phys. Lett.* 2007, *448*, 183−188.

(24) Karton, A.; Kettner, M.; Wild, D. A. Sneaking up on the Criegee Intermediate from Below: Predicted Photoelectron Spectrum of the CH₂OO⁻ Anion and W3-F12 Electron Affinity of CH₂OO. *Chem. Phys. Lett.* 2013, *585*, 15−20.

(25) Kalinowski, J.; Rasanen, M.; Heinonen, P.; Kilpelainen, I.; Gerber, R. B. Isomerization and Decomposition of a Criegee Intermediate in the Ozonolysis of Alkenes: Dynamics Using a Multireference Potential. *Angew. Chem., Int. Ed.* 2014, *53*, 265−268.

(26) Jiang, B.; Guo, H. Permutation Invariant Polynomial Neural Network Approach to Fitting Potential Energy Surfaces. *J. Chem. Phys.* 2013, *139*, 054112.

(27) Li, J.; Jiang, B.; Guo, H. Permutation Invariant Polynomial Neural Network Approach to Fitting Potential Energy Surfaces. II. Four-Atomic Systems. *J. Chem. Phys.* 2013, *139*, 204103.

(28) Bowman, J. M.; Carter, S.; Huang, X. Multimode: A Code to Calculate Rovibrational Energies of Polyatomic Molecules. *Int. Rev. Phys. Chem.* 2003, *22*, 533−549.

(29) Adler, T. B.; Knizia, G.; Werner, H.-J. A Simple and Efficient CCSD(T)-F12 Approximation. *J. Chem. Phys.* 2007, *127*, 221106.

(30) Knizia, G.; Adler, T. B.; Werner, H.-J. Simplified CCSD(T)-F12 Methods: Theory and Benchmarks. *J. Chem. Phys.* 2009, *130*, 054104.

(31) *MOLPRO2012*. Molpro, Version 2012.1, a Package of Ab Initio Programs. Werner, H.-J.; Knowles, P. J.; Knizia, G.; Manby, F. R.; M. Schütz, et al. See http://www.Molpro.Net. .

(32) Braams, B. J.; Bowman, J. M. Permutationally Invariant Potential Energy Surfaces in High Dimensionality. *Int. Rev. Phys. Chem.* 2009, *28*, 577−606.

(33) Bowman, J. M.; Czakó, G.; Fu, B. High-Dimensional Ab Initio Potential Energy Surfaces for Reaction Dynamics Calculations. *Phys. Chem. Chem. Phys.* 2011, *13*, 8094−8111.

(34) Li, J.; Wang, Y.; Jiang, B.; Ma, J.; Dawes, R.; Xie, D.; Bowman, J. M.; Guo, H. Communication: A Chemically Accurate Global Potential Energy Surface for the HO + CO → H + CO₂ Reaction. *J. Chem. Phys.* 2012, *136*, 041103.

(35) Frisch, M. J.; Trucks, G. W.; Schlegel, H. B.; Scuseria, G. E.; Robb, M. A.; Cheeseman, J. R.; Scalmani, G.; Barone, V.; Mennucci, B.; Petersson, G. A.; Nakatsuji, H.; Caricato, M.; Li, X.; Hratchian, H. P.; Izmaylov, A. F.; Bloino, J.; Zheng, G.; Sonnenberg, J. L.; Hada, M.; Ehara, M.; Toyota, K.; Fukuda, R.; Hasegawa, J.; Ishida, M.; Nakajima, T.; Honda, Y.; Kitao, O.; Nakai, H.; Vreven, T.; Montgomery, J., J. A.; Peralta, J, E.; Ogliaro, F.; Bearpark, M.; Heyd, J. J.; Brothers, E.; Kudin, K. N.; Staroverov, V. N.; Kobayashi, R.; Normand, J.; Raghavachari, K.; Rendell, A.; Burant, J. C.; Iyengar, S. S.; Tomasi, J.; Cossi, M.; Rega, N.; Millam, N. J.; Klene, M.; Knox, J. E.; Cross, J. B.; Bakken, V.; Adamo, C.; Jaramillo, J.; Gomperts, R.; Stratmann, R. E.; Yazyev, O.; Austin, A. J.; Cammi, R.; Pomelli, C.; Ochterski, J. W.; Martin, R. L.; Morokuma, K.; Zakrzewski, V. G.; Voth, G. A.; Salvador, P.; Dannenberg, J. J.; Dapprich, S.; Daniels, A. D.; Farkas, Ö.;

Foresman, J. B.; Ortiz, J. V.; Cioslowski, J.; Fox, D. J. *Gaussian09*, Gaussian, Inc.: Wallingford, CT, 2009.

(36) Li, J.; Chen, J.; Zhang, D. H.; Guo, H. Quantum and Quasi-Classical Dynamics of the OH + CO → H + CO₂ Reaction on a New Permutationally Invariant Neural Network Potential Energy Surface. *J. Chem. Phys.* 2014, *140*, 044327.

(37) Li, J.; Guo, H. A Nine-Dimensional Global Potential Energy Surface for NH₄(X²A₁) and Kinetics Studies on the H + NH₃ ↔ H₂ + NH₂ Reaction. *Phys. Chem. Chem. Phys.* 2014, *16*, 6753−6763.

(38) Li, A.; Guo, H. A Nine-Dimensional Ab Initio Global Potential Energy Surface for the H₂O⁺ + H₂ → H₃O⁺ + H Reaction. *J. Chem. Phys.* 2014, *140*, 224313.

(39) Xie, Z.; Bowman, J. M. Permutationally Invariant Polynomial Basis for Molecular Energy Surface Fitting Via Monomial Symmetrization. *J. Chem. Theor. Comput.* 2010, *6*, 26−34.

(40) Raff, L. M.; Komanduri, R.; Hagan, M.; Bukkapatnam, S. T. S. *Neural Networks in Chemical Reaction Dynamics*; Oxford University Press: Oxford, U.K., 2012.

(41) Wang, Y.; Huang, X.; Shepler, B. C.; Braams, B. J.; Bowman, J. M. Flexible, Ab Initio Potential, and Dipole Moment Surfaces for Water. I. Tests and Applications for Clusters up to the 22-Mer. *J. Chem. Phys.* 2011, *134*, 094509.

(42) Watson, J. K. G. Simplification of Molecular Vibration-Rotation Hamiltonian. *Mol. Phys.* 1968, *15*, 479−490.

(43) Bowman, J. M. The Self-Consistent-Field Approach to Polyatomic Vibrations. *Acc. Chem. Res.* 1986, *19*, 202−208.

(44) Ratner, M. A.; Gerber, R. B. Excited Vibrational States of Polyatomic Molecules: The Semiclassical Self-Consistent-Field Approach. *J. Phys. Chem.* 1986, *90*, 20−30.

(45) Carter, S.; Bowman, J. M. The Adiabatic Rotation Approximation for Rovibrational Energies of Many-Mode Systems: Description and Tests of the Method. *J. Chem. Phys.* 1998, *108*, 4397−4404.

(46) Carter, S.; Bowman, J. M.; Handy, N. C. Extensions and Tests of "Multimode": A Code to Obtain Accurate Vibration/Rotation Energies of Many-Mode Molecules. *Theor. Chem. Acc.* 1998, *100*, 191−198.

(47) Burcl, R.; Carter, S.; Handy, N. C. Infrared Intensities from the Multimode Code. *Chem. Phys. Lett.* 2003, *380*, 237−244.

(48) Dawes, R.; Lolur, P.; Li, A.; Jiang, B.; Guo, H. Communication: An Accurate Global Potential Energy Surface for the Ground Electronic State of Ozone. *J. Chem. Phys.* 2013, *139*, 201103.

(49) Ayouz, M.; Babikov, D. Global Permutationally Invariant Potential Energy Surface for Ozone Forming Reaction. *J. Chem. Phys.* 2013, *138*, 164311.

(50) Tyuterev, V. G.; Kochanov, R. V.; Tashkun, S. A.; Holka, F.; Szalay, P. G. New Analytical Model for the Ozone Electronic Ground State Potential Surface and Accurate Ab Initio Vibrational Predictions at High Energy Range. *J. Chem. Phys.* 2013, *139*, 134307.

(51) Watts, J.; Bartlett, R. J. Coupled-Cluster Calculations of Structure and Vibrational Frequencies of Ozone: Are Triple Excitations Enough? *J. Chem. Phys.* 1998, *108*, 2511.

2369

dx.doi.org/10.1021/jz501059m | *J. Phys. Chem. Lett.* 2014, 5, 2364−2369